Journal of Catalysis 261 (2009) 224–231

Contents lists available at ScienceDirect

Journal of Catalysis

www.elsevier.com/locate/jcat

Remarkable particle size effect in Rh-catalyzed enantioselective hydrogenations

Fatos Hoxha, Niels van Vegten, Atsushi Urakawa, Frank Krumeich, Tamas Mallat, Alfons Baiker *

Institute for Chemical and Bioengineering, Department of Chemistry and Applied Biosciences, ETH Zurich, Hönggerberg, HCI, CH-8093 Zurich, Switzerland

ARTICLE INFO

Article history:
Received 11 November 2008
Revised 2 December 2008
Accepted 3 December 2008
Available online 20 December 2008

Keywords:
Rhodium
Ethyl pyruvate
Ethyl 3-methyl-2-oxobutyrate
Cinchonidine
Quinine
Asymmetric hydrogenation
Particle size effect
Structure sensitivity

ABSTRACT

A series of 0.5–4.3 wt% Rh/Al_2O_3 catalysts were prepared by flame synthesis. STEM indicated relatively narrow particle size distributions for all catalysts and the mean particle size increased almost linearly with the Rh content in the range 0.96–1.65 nm. A DRIFTS study of CO adsorption on as prepared Rh/Al_2O_3 and after heat treatment in hydrogen at 400 °C revealed that there was no Rh oxide present at the catalyst surface after the high temperature reduction, which procedure is commonly used prior to enantioselective hydrogenation. In the hydrogenation of ethyl pyruvate and ethyl 3-methyl-2-oxobutyrate the cinchona-modified 4.3 wt% Rh/Al_2O_3 gave considerably higher ee than those achieved with the best known Rh catalyst. A decrease of the metal loading and thus the mean Rh particle size, led to a loss of ee to (*R*)-lactate by a factor of up to seven at 1 bar and up to two at 10–100 bar. Our interpretation is that the performance of Rh/Al_2O_3 is strongly distorted at atmospheric pressure by catalyst deactivation due to the Al_2O_3-catalyzed aldol condensation of the substrate. During the fast reactions at 100 bar the contribution of strongly adsorbed impurities is small and the variation of ee is mainly due to an intrinsic particle size effect. The structure sensitivity observed under optimal conditions, at high surface hydrogen concentration, is mainly due to steric effects: a small, ca. 1 nm Rh particle cannot accommodate the enantiodifferentiating diastereomeric substrate–modifier complex and the hydrogenation on its surface leads to racemic product. A practical conclusion is that there is no advantage of using small nanoparticles and low metal loading in the enantioselective hydrogenation of α-ketoesters.

1. Introduction

In the enantioselective hydrogenation of activated ketones, chirally modified Rh is characterized by moderate chemo- and enantioselectivities [1–7], not comparable to that of the Pt–cinchona system [8–11]. An exception is the hydrogenation of hydroxyketones on cinchonidine (CD)-modified Rh/Al_2O_3 with up to 80% ee [12]. Even in this reaction, however, the reaction rate was low and high modifier/substrate molar ratio was necessary, mainly due to the competing hydrogenation and destruction [13,14] of the modifier itself. Several attempts have been made to improve the performance of Rh and to broaden the scope of suitable substrates. Recently, in the hydrogenation of ketopantolactone Rh/Al_2O_3 in the presence of β-isocinchonine gave 68% ee and in this facile reaction only a low modifier/substrate ratio was necessary [15]. In the above studies the research aimed at finding the appropriate combination of catalyst, modifier, and the reaction conditions, without a profound analysis on the role of catalyst structure, metal particle size, and surface morphology.

It is well established that the catalytic properties may be strongly influenced by the size of metal particles [16–18]. The classical calculations from Boronin and Poltorak [19] and van Hardeveld and Hartog [20] showed that the biggest changes of proportions between facets, edges, corners, and micro-defects at the surface occur between 1 and 5 nm. Above 5 nm the metal–support interaction tend to decrease rapidly, making the catalyst of little value for studying the structural effects [21]. Depending on whether or not the turnover frequency (TOF) is affected by the structure of the particle surface, Boudart [22] coined the terms structure-sensitive or structure-insensitive reaction.

Hydrogenation of unsaturated hydrocarbons on Pd is an early and thoroughly investigated case of structure sensitive reactions [23,24]. Hydrogenation of alkenes is barely sensitive to the metal particle size, while strong dependence of rate and selectivity was observed in the partial hydrogenation of alkadienes and alkynes.

There are numerous studies [25–28] indicating some structure sensitivity of asymmetric hydrogenation reactions on Pt, Pd, Ni, Ru, and Ir, but systematic studies with properly designed catalysts are rare and the presence of unidentified surface impurities may blur the real correlation [29,30]. According to an early report on the hydrogenation of ethyl pyruvate on CD-modified Pt/Al_2O_3 [31], both initial rate and enantioselectivity increased with increasing Pt par-

* Corresponding author.
E-mail address: baiker@chem.ethz.ch (A. Baiker).

0021-9517/$ – see front matter
doi:10.1016/j.jcat.2008.12.002

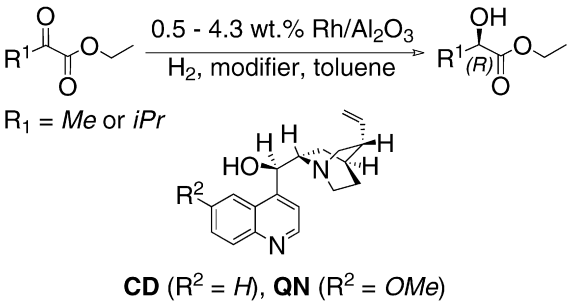

Scheme 1. Hydrogenation of ethyl pyruvate and ethyl 3-methyl-2-oxobutyrate on Rh/Al_2O_3 in the presence of quinine (QN) and cinchonidine (CD), respectively.

ticle size up to 3–4 nm. However, due to the different preparation conditions (Pt precursor, reducing agent, etc.) a significant effect of surface impurities on the catalyst performance cannot be excluded. In another study of pyruvate hydrogenation [32], the metal particle size of Pt/graphite was increased by sintering at elevated temperature in hydrogen. As a result, the ee increased to some extent but then dropped when the sintering temperature exceeded 700 K, due to contamination of Pt with graphite.

Beside the variation of surface impurities, a too broad metal particle size distribution may also hinder to draw unambiguous conclusions on the particle size effect [32,33]. In some other cases the enantioselectivities are low, far from the optimum, and it is questionable whether the observed correlation between metal particle size and enantioselectivity is valid also at close to the optimum conditions of the reaction [34,35].

Here we report for the first time the effect of particle size on the enantioselectivity of chirally modified Rh. The flame made Rh/Al_2O_3 catalyst series, with a particle size distribution from 0.6 to 2.4 nm, has already been used for studying the chemoselectivity in the hydrogenation of an aromatic ketone [36]. In the present study, hydrogenation of the α-ketoesters ethyl lactate and ethyl 3-methyl-2-oxobutyrate was chosen as test reactions and the catalysts were modified with CD or quinine (QN), respectively (Scheme 1).

2. Experimental

2.1. Materials

The substrates ethyl pyruvate (Acros, 98%, 0.02% ethyl lactate after distillation) and ethyl 3-methyl-2-oxobutyrate (Aldrich, 97%) were carefully distilled in vacuum before use. Other chemicals were used as received: cinchonidine (CD) (Fluka, $\geqslant$98% alkaloid), quinine (QN) (Fluka, ca. 99% alkaloid), toluene (Aldrich, anhydrous 99.8%), rhodium(III) acetylacetonate (Acros, 97%), aluminum(III) acetylacetonate (ABCR, 99%), acetic acid (Fluka, analytical grade), methanol (Fluka, analytical grade).

The preparation of Rh/Al_2O_3 catalysts with the flame spray pyrolysis technique is described in previous reports [36,37]. Shortly, the appropriate amounts of Rh and Al precursors were dissolved in an acetic acid/methanol 1/1 (volume ratio) mixture. The Al concentration was always 0.39 M. The solution was pumped through a capillary at a rate of 5 mL/min and nebulized with 5 L_n/min O_2, and the resulting spray was ignited by a circular supporting methane/oxygen flame (1.0/0.6 L_n/min), resulting in an approximately 6 cm long flame. Particles were collected on a cooled Whatman GF/D filter (257 mm diameter). A Busch SV 1040C vacuum pump aided in particle recovery.

The metal content of the catalysts was determined with inductively coupled plasma atomic emission spectroscopy (ICP-AES) technique (by Alab AG, Switzerland) after dissolution in *aqua regia*. As shown in Table 1, the Rh contents were mostly lower than the nominal value, with a deviation of up to 32% (rel.). The water content of the catalysts did not exceed 10 wt%.

Table 1
Nominal and measured Rh content of Rh/Al_2O_3 catalysts (ICP-AES technique after dissolution in *aqua regia*).

Nominal Rh content (wt%)	Measured Rh content (wt%)
0.5	0.5
1	0.8
2	1.4
3	2.5
4	3.5
5	4.3

2.2. Catalytic hydrogenation

The catalyst was always reduced at elevated temperature priore to use. According to the standard procedure, the catalyst was heated under flowing nitrogen up to 400 °C in 30 min, followed by a reduction in flowing hydrogen for 60 min at the same temperature, and finally cooling down in hydrogen in 30 min.

Hydrogenations at atmospheric pressure were carried out in a 100-ml glass reactor equipped with magnetic stirrer, septum for sample collection or substrate addition, and an in and outlet line for gas flowing. To avoid the contact of the freshly reduced catalyst with air, the reductive heat treatment and the hydrogenation reaction were made in the same reactor. After introducing the solvent and the modifier into the reactor containing the freshly reduced catalyst under hydrogen at room temperature, the mixture was stirred for 1 min. The reaction was started by introducing the substrate and immediately switching on the stirring.

The same reactor was used to study the Al_2O_3-catalyzed degradation of ethyl pyruvate. The conditions were identical to those of catalytic hydrogenation but the Rh/Al_2O_3 catalyst was replaced with the appropriate amount of Al_2O_3. The flame made Al_2O_3 (specific surface area 267 m^2/g) was heated at 400 °C under nitrogen for 1 h and finally cooled down to room temperature. To the activated Al_2O_3 a solution of ethyl pyruvate and tetradecane (internal standard) in toluene were introduced and the reaction started by switching on the stirring. The nitrogen atmosphere was maintained throughout the experiment.

The hydrogenations at elevated pressure were carried out in a 25 ml stainless steel Parr autoclave equipped with a 16 ml glass liner and a PTFE cover, and a magnetic stirrer. The autoclave was equipped also with a valve for sample collection or substrate addition. The treatment of the catalyst was carried out in a fix-bed reactor following the standard procedure. At the end, the freshly reduced catalyst was purged with nitrogen for 60 min at room temperature to remove the excess of hydrogen and then transferred immediately to the autoclave.

In all experiments, the Rh/modifier/substrate molar ratios were kept constant at 1/3.7/189. In the hydrogenations at elevated pressure, the proper amount of Rh/Al_2O_3 containing 2.43 μmol Rh, 9 μmol modifier, 0.46 mmol substrate, and 5 ml solvent were stirred magnetically (1000 rpm) at room temperature for 60 min. The pressure was held at a constant value with a constant pressure regulator valve. In the hydrogenations at atmospheric pressure, 9.72 μmol Rh catalyst, 36 μmol modifier, 1.84 mmol substrate, and 15 ml solvent were stirred magnetically (1000 rpm) at room temperature for 120 min.

The conversion and enantioselectivity (ee) were determined by GC analysis, using an HP 6890 gas chromatograph and a Chirasil-DEX CB (Chrompack 7502 25 m × 0.25 mm × 0.25 μm) capillary column. All experiments were carried out at least twice and the average values are shown in the figures. In all experiment the

(*R*)-enantiomer was formed in excess without any detectable side product. The estimated standard deviation of ee is about ±0.5%.

2.3. Characterization of the catalysts

The scanning transmission electron microscopic (STEM) analysis was performed on a Tecnai F30 microscope (FEI, field emission cathode, operated at 300 kV). The material was dispersed in ethanol and some drops were deposited onto a perforated carbon foil supported on a copper grid. STEM images were recorded with a high-angle annular dark field (HAADF) detector, using almost exclusively incoherently scattered electrons (Rutherford scattering) to obtain images with atomic number (*Z*) contrast [38]. The mean Rh particle size d_{VS} was calculated based on a minimum of 200 particles using the following equation:

$$d_{VS} = \sum_i n_i d_i^3 \Big/ \sum_i n_i d_i^2,$$

were n_i is the number of particles with diameter d_i.

Diffuse reflectance infrared Fourier transform spectroscopy (DRIFTS) was used to study the CO adsorption on Rh/Al_2O_3. The analysis was carried out at 297 K with an EQUINOX 55 spectrometer (Bruker Optics) equipped with a liquid nitrogen-cooled HgCdTe detector. Multiple samples (max. 4), separated by quartz wool, were placed without dilution in a plug–flow DRIFTS cell [39], allowing identical experimental conditions for all samples. The off gas of the cell was analyzed by a mass spectrometer. Spectra were collected by averaging 200 scans at 4 cm^{-1} resolution. The standard treatment procedure mentioned above was used to reduce the catalyst (flowing H_2, 20 ml/min), in this case with argon (Ar) as inert gas. CO adsorption was monitored over 60 min in flowing 10 vol% CO/Ar (5 ml/min), followed by flowing Ar (20 ml/min) for 30 min.

3. Results and discussion

3.1. Electron microscopy

The particle size distribution of the six Rh/Al_2O_3 catalysts was determined by scanning transmission electron microscopy (STEM). In all cases Rh was highly dispersed with a relatively narrow particle size distribution, particularly for the three lowest metal loadings (Fig. 1). The mean particle size increased monotonously in the range 0.96–1.65 nm with increasing Rh loading. The straightforward correlation between the mean particle size and the Rh content is shown in Fig. 2. The catalysts were pretreated according to the standard procedure at elevated temperature prior to STEM investigation; hence these data can be directly related to the hydrogenation rates and selectivities. A comparison of the samples before and after pretreatment at 400 °C revealed no major structural changes. For example, the mean Rh particle size of the freshly prepared 2.5 wt% Rh/Al_2O_3 catalyst increased by less than 10% during the reductive pretreatment.

3.2. IR study of CO adsorption

The DRIFT spectra of CO adsorbed on the flame made 4.3 wt% Rh/Al_2O_3 catalyst (both as-received and after reduction at 400 °C) have already been published [36]. Here we extended the investigation to the whole catalyst series in order to gain insight into the oxidation state of rhodium species after the standard reductive treatment. Since only the metallic Rh surface sites are active in the hydrogenation reactions, determination of the oxidation state of Rh is inevitable to understand the performance of these catalysts. The standard catalyst treatment procedure prior to hydrogenations was used here also: the samples were reduced in flowing hydrogen at 400 °C and the exhaust gas was analyzed using mass spectrometry. The stabilized reduced state of the catalyst was reached within 40 min (the concentration of the exhaust gas mixture was constant showing low water content).

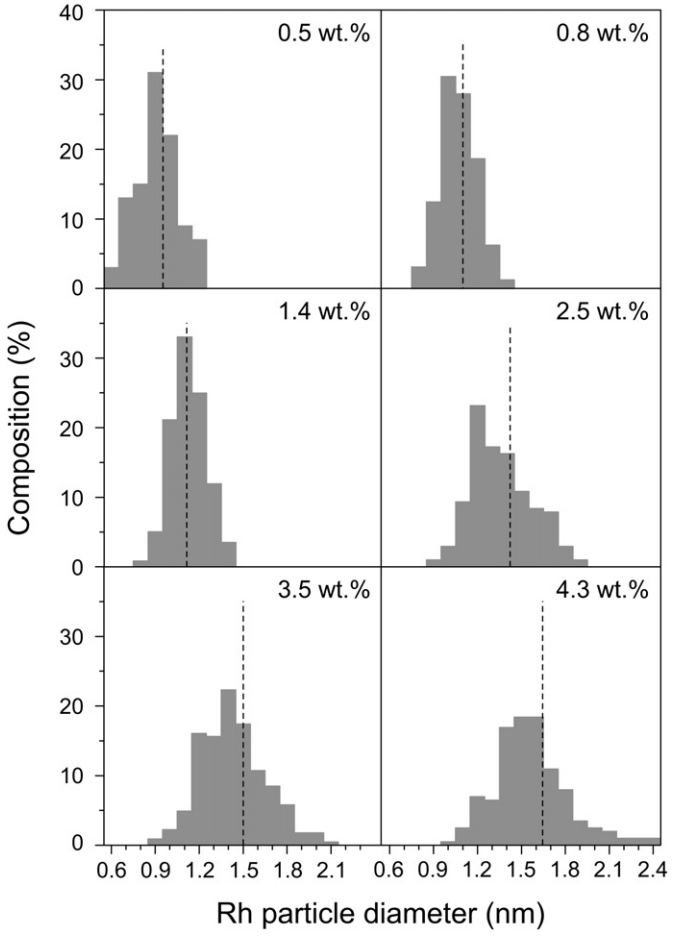

Fig. 1. Particle size distribution of Rh/Al_2O_3 catalysts prereduced at 400 °C in H_2. The dashed vertical lines represent the mean diameter d_{VS}.

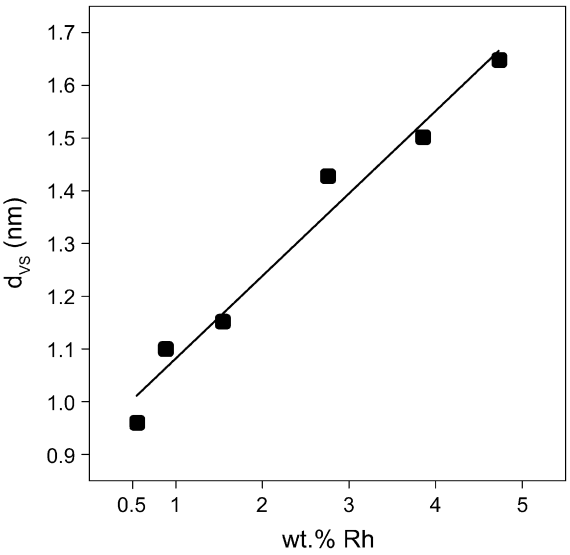

Fig. 2. Influence of Rh loading on the mean size of metallic crystallites. Samples were prereduced at 400 °C in H_2.

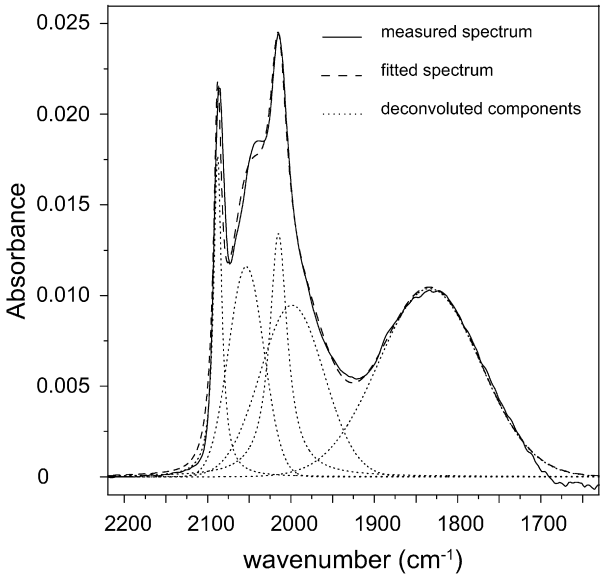

Fig. 3. IR spectrum of the 0.5 wt% Rh/Al_2O_3, prereduced at 400 °C in H_2, and the deconvoluted components of the CO bands.

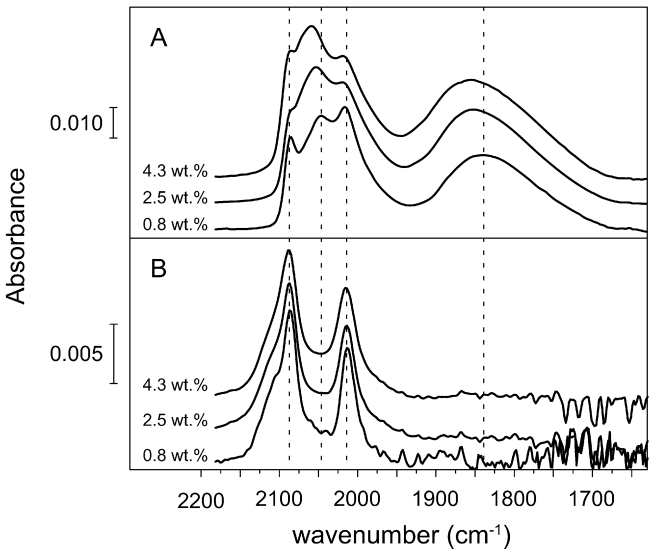

Fig. 4. Typical DRIFT spectra of CO adsorption on Rh/Al_2O_3 samples, prereduced at 400 °C in H_2 (top) and as received (bottom).

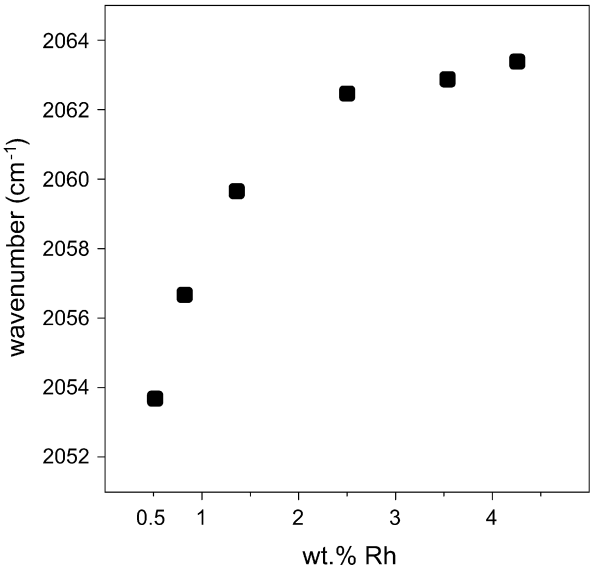

Fig. 5. Shift of the linear Rh^0–CO band with increasing Rh loading. Data are extracted from the deconvoluted IR spectra of CO adsorption on reduced Rh/Al_2O_3 catalysts.

The DRIFT spectrum of CO adsorbed on the reduced 0.5 wt% Rh/Al_2O_3 catalyst is shown in Fig. 3. Three kinds of CO bands were identified in the IR spectra. The broad band (1832–1835 cm^{-1}) is attributed to the multi-bonded CO species Rh_n^0 (–CO, $n \geqslant 2$). The bands between 2000 and 2100 cm^{-1} are associated with two species: a doublet corresponds to the symmetric (2086 cm^{-1}) and asymmetric (2015 cm^{-1}) stretch of gem-dicarbonyl Rh^+–$(CO)_2$ dimer vibrations and the band at 2053–2063 cm^{-1} is assigned to linear Rh^0–CO species [40–48]. Figs. 4 and 5 illustrate that with increasing Rh content of the catalysts both bands corresponding to linear and bridged CO species on Rh_n^0 sites are enhanced in relative intensity and shifted to higher wavenumbers. The latter correlation indicates increasing metal particle size [48–51], in line with the STEM measurements (Fig. 2) that revealed a positive correlation between Rh loading and the mean metal particle size. The bands of the carbonyl species have a constant wavenumber, independent of the Rh loading [46,50], and thus the band positions (2086 and 2015 cm^{-1}) were set constant during the spectral deconvolution procedure.

In the infrared spectra of the unreduced samples the bands corresponding to the gem-dicarbonyl species Rh^+–$(CO)_2$ (2015 and 2086 cm^{-1}) were dominant. The shoulder at ca. 2110 cm^{-1} corresponds to linearly bonded CO on Rh^{2+}, typical for oxidized rhodium [49,52]. Importantly, this band was not detectable on the reduced samples.

The presence of Rh^+ species in the IR spectra is commonly attributed to interaction with gaseous CO. The Rh^+–$(CO)_2$ species can be formed during CO adsorption by the oxidation of Rh^0 sites involving the hydroxyls groups on the surface of the support [53–55]. Van't Blik et al. [56] studied the coordination of Rh atoms on a 0.57 wt% Rh/Al_2O_3 catalyst with EXAFS technique. They proved that the adsorption of CO causes a significant disruption of the local coordination environment of the Rh_x^0 crystallites, leading to the formation of isolated, atomically dispersed Rh^+ sites localized and stabilized on the Al_2O_3 surface [53,54]. The presence of the Rh^+–$(CO)_2$ bands in the IR spectra of the unreduced catalyst may be explained by reduction of the oxidized species Rh^{n+} ($n \geqslant 2$) with the involvement of the OH groups on the Al_2O_3 surface [57] or by the adsorbant CO itself [54].

Another feasible explanation for the presence of cationic species is the formation of Rh aluminate ($Rh(AlO_2)_y$ [58]) during the flame spray catalyst synthesis. The presence of $Rh(AlO_2)_y$ is typical for Rh/Al_2O_3 catalysts treated at elevated temperature under an oxygen atmosphere [58–60]. Formation of $Rh(AlO_2)_y$ has been considered the origin of the deactivation of Rh/Al_2O_3 in oxidation reactions. Their activity may partially be restored by an appropriate reductive treatment at temperatures above 600 °C [59,61–64], but the conditions in the reductive treatment used in the present study are too mild for this type of regeneration.

It was shown that the fraction of Rh^+–$(CO)_2$ species created during CO adsorption decreased with increasing rhodium particle size [40,48,62], and a similar correlation may be expected for Rh aluminate formation. In our study based on the deconvoluted spectra, the ratio of Rh_x^0 to cationic Rh^+ species is 2–2.5 at low Rh content (0.5–1.4 wt% Rh/Al_2O_3) and 9–18 at higher Rh loadings (Fig. 6).

Despite of the well known chemical interaction of CO and Rh/Al_2O_3 that complicates the adsorption study, the DRIFT measurements prove that (i) the Rh_x^0 particle size increases monotonously with the Rh loading, (ii) there is no rhodium oxide present

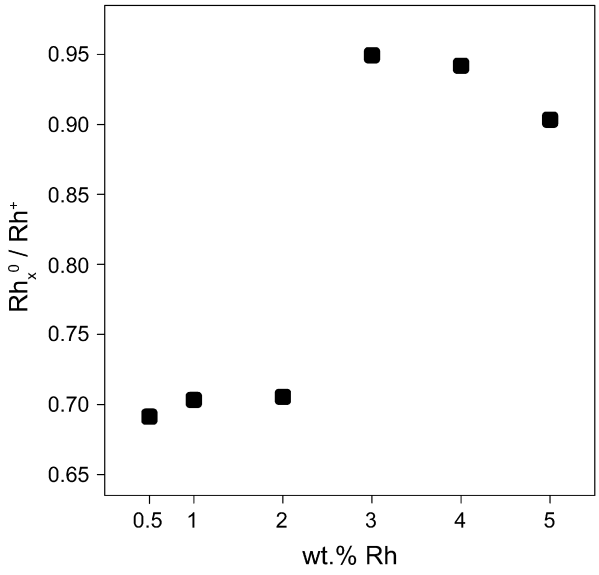

Fig. 6. Ratio of metallic (Rh_x^0) to cationic (Rh^+) rhodium species in Rh/Al_2O_3 catalysts, as determined from the DRIFT spectra of CO adsorption.

after the standard reductive pretreatment procedure at 400 °C, and (iii) the existence of ionic Rh species as Rh aluminate in the flame made catalysts cannot be excluded.

3.3. Enantioselective hydrogenation

Based on former observations in the Rh-catalyzed hydrogenation of activated ketones [15], the best substrate-modifier-solvent systems were chosen here to test the performance of the flame made Rh/Al_2O_3 catalysts. In order to avoid the re-oxidation of the metallic Rh particles during transfer of the catalyst from the fixed bed reactor commonly used for catalyst prereduction to the autoclave, here we used a special glass reactor for both steps, the catalyst pretreatment at 400 °C and the enantioselective hydrogenation of α-ketoesters at room temperature and atmospheric pressure.

Variation of enantioselectivity and reaction rate (expressed as TOF) in the hydrogenation of ethyl pyruvate on quinine-modified Rh/Al_2O_3 are plotted in Fig. 7 as a function of mean metal particle size. The TOF values were calculated based on the STEM-derived Rh dispersions [46,65]; i.e. the reaction rate is related to the fraction of surface Rh atoms. The ees determined at a relatively low ($9 \pm 2\%$) conversion show that the increase of the Rh mean particle size from 0.96 to 1.65 nm induced the increase of ee from 7 to 47%. Similar trend was observed after 2 h reaction time, where the ee increased from 11 to 53% and the yield to ethyl lactate grew from 15 to 56% (Fig. 7a). The increase of the mean particle size from 0.96 to 1.65 nm led to a nine fold enhancement of the reaction rate at $9 \pm 2\%$ conversion and up to five fold enhancement after 2 h reaction time (Fig. 7b).

Interpretation of the surprisingly big changes in rate and enantioselectivity needs caution. It is well known that hydrogenation of α-ketoesters is accompanied by extensive side reactions [66]. A dominant side reaction is the aldol reaction of the activated ketone leading to strongly adsorbing dimers and oligomers. This side reaction is catalyzed by the basic quinuclidine N of the modifier, the basic sites on the Al_2O_3 support [67,68], and the metal surface [69,70]. A simple way to suppress the base-catalyzed aldol reaction is to use an acidic solvent (acetic acid), but in our case it is not a good solution due to the poor selectivity of Rh in this medium [15]. In all experiments, the Rh/modifier/substrate molar ratios were kept constant in order to obtain comparable results. An obvious consequence of this approach is that variation

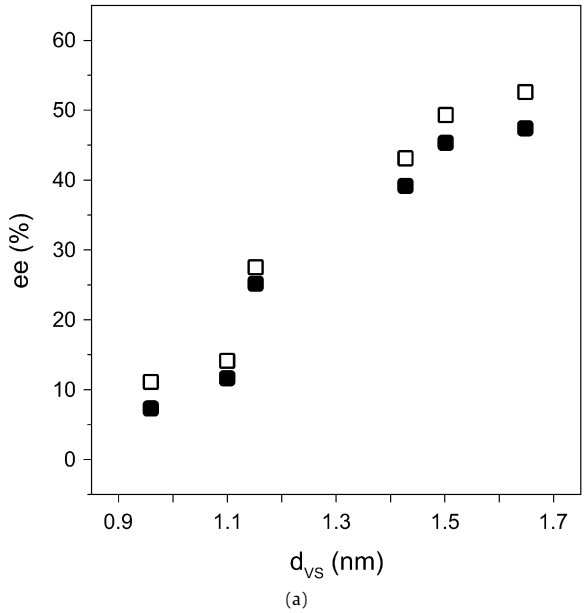

Fig. 7. Influence of Rh mean particle size on the enantioselectivity and reaction rate in the hydrogenation of ethyl pyruvate to (*R*)-ethyl lactate over quinine-modified Rh/Al_2O_3 catalysts; standard conditions, toluene, 1 bar, 24 °C; filled symbols: data at $9 \pm 2\%$ conversion, open symbols: data after 2 h reaction time.

of the Rh loading of the catalysts leads to changes in the ethyl pyruvate/Al_2O_3 molar ratio, in our case from 0.94 to 9.4 for the lowest and highest Rh loading, respectively. To prove the significance of the Al_2O_3-catalyzed aldol reaction under the conditions applied here, we repeated the reaction in Fig. 7 with the 0.5 wt% Rh/Al_2O_3 catalyst but replaced the catalyst with the appropriate amount of flame made Al_2O_3 and the hydrogen with nitrogen. The disappearance of ethyl pyruvate in dry toluene as solvent is shown in Fig. 8. The rapid drop of pyruvate concentration in solution in the first few minutes is attributed to adsorption on the high surface area support. The slower but still considerable conversion of ethyl pyruvate is mainly due to the aldol condensation, as shown previously by ATR-IR spectroscopy [67,68]. No (volatile) products were detectable by GC analysis. Oligomers that are formed by aldol condensation may strongly adsorb on the catalyst surface including the metal particles and diminish the reaction rate and enantiose-

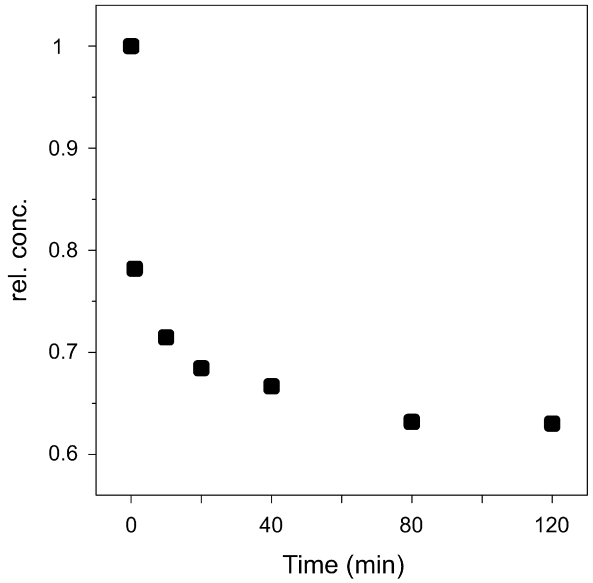

Fig. 8. Ethyl pyruvate consumption in the presence of Al_2O_3, standard conditions, toluene, 1 bar, 24 °C, N_2 atmosphere.

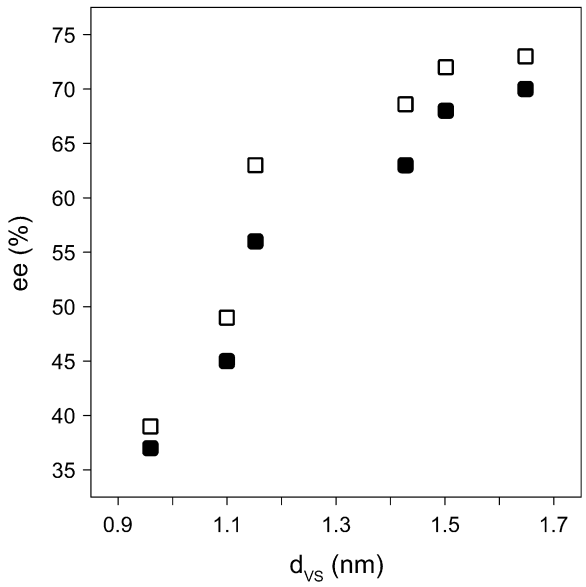

Fig. 9. Influence of mean Rh particle size on the enantioselectivity in the hydrogenation of ethyl pyruvate to (*R*)-ethyl lactate with quinine-modified Rh/Al_2O_3 catalysts; standard conditions, toluene, 24 °C; filled symbols: data at 10 bar, open symbols: data at 100 bar.

lectivity. It has been shown for the hydrogenation of ethyl pyruvate on Pt/Al_2O_3 in toluene that non-volatile impurities in the substrate diminish the reaction rate by a factor of up to 11 and the enantioselectivity by 1–8% [71]. Assuming that Pt/Al_2O_3 and Rh/Al_2O_3 behave similarly in this respect, we can conclude that the striking variation in reaction rates in Fig. 7a cannot simply be considered as a particle size effect but it is mainly due to the different extent of catalyst deactivation. On the other hand, the changes in enantioselectivity are probably less affected by the impurities.

To prove this assumption we repeated the experiments shown in Fig. 7 at higher pressures. High surface hydrogen concentration suppresses the initial step of aldol reaction, the abstraction of an α-H atom on the metal surface. In addition, it accelerates the hydrogenation reaction while the rate of the base-catalyzed aldol reaction remains the same. The hydrogenation experiments carried out at 10 and 100 bar (Fig. 9) reveal that variation of the ee with Rh particle size is smaller but still considerable. Hydrogenations at 100 bar give 4–8% higher ees than the values at 10 bar, and full conversion was achieved with all catalysts in 1 h, while at 10 bar the conversions were in the range 70–100%. In the best case 73% ee was obtained with the highest Rh loading (at 1.65 nm Rh mean particle size). It has been shown that high pressure (high surface hydrogen concentration) improves the enantioselectivity in the hydrogenation of activated ketones on supported Rh [5,15].

Our interpretation of the results in Figs. 7–9 is that the performance of Rh/Al_2O_3 is strongly distorted at atmospheric pressure by catalyst deactivation, but the similar enantioselectivities at 10 and 100 bar indicate that at high pressure the variation of ee is mainly due to an intrinsic particle size effect and the contribution of strongly adsorbed impurities is probably minor.

In the hydrogenation of ethyl 3-methyl-2-oxobutyrate at 10 bar in the presence of CD the difference between the highest and lowest ee was only 10% (Fig. 10). The conversion in 1 h reaction time increased from 70 to 100% with increasing particle size.

The potential of the flame spray catalyst synthesis is illustrated by the best enantioselectivities achieved in the hydrogenation of ethyl pyruvate and ethyl 3-methyl-2-oxobutyrate: the 4.3 wt% Rh/Al_2O_3 catalyst gave 24 and 17% higher ees, respectively, than those provided by the best commercial catalyst (Engelhard 4759) under the same reaction conditions [15].

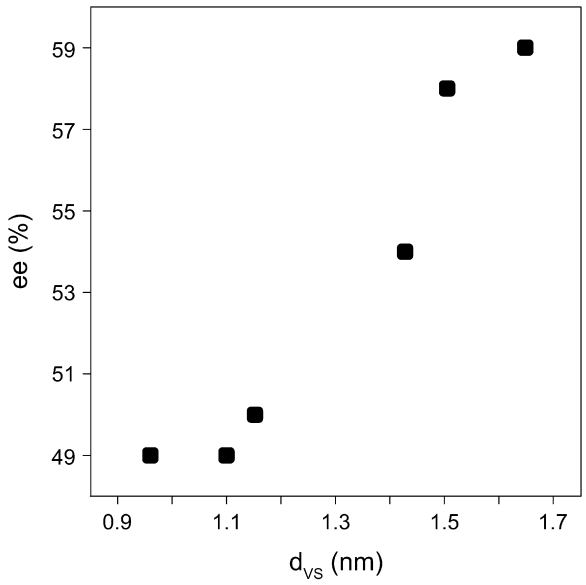

Fig. 10. Influence of mean Rh particle size on the enantioselectivity in the hydrogenation of ethyl 3-methyl-2-oxobutyrate with cinchonidine-modified Rh/Al_2O_3 catalysts; standard conditions, toluene, 10 bar, 24 °C.

3.4. Origin of particle size effect

As mentioned in the introduction, there are numerous catalytic and theoretical studies addressing the particle size effect in heterogeneous catalysis [16,17]. Various explanations have been forwarded, putting the emphasis on the electronic [18] or the geometric [72] parameters. Regarding the electronic properties, the critical size above which the band structure appears is about 2 nm. At a lower size, the d-band becomes narrower with the appearance of discrete levels, leading to electron deficiency of small particles [17,73], where the small metal particles bind their core electrons more tightly. Regarding the geometrical features, the idealized topology of the surface shows big changes up to about 5 nm [20], due to variations in the proportion of facets, edges, steps, corners, and defects. The metal–support interaction may also play

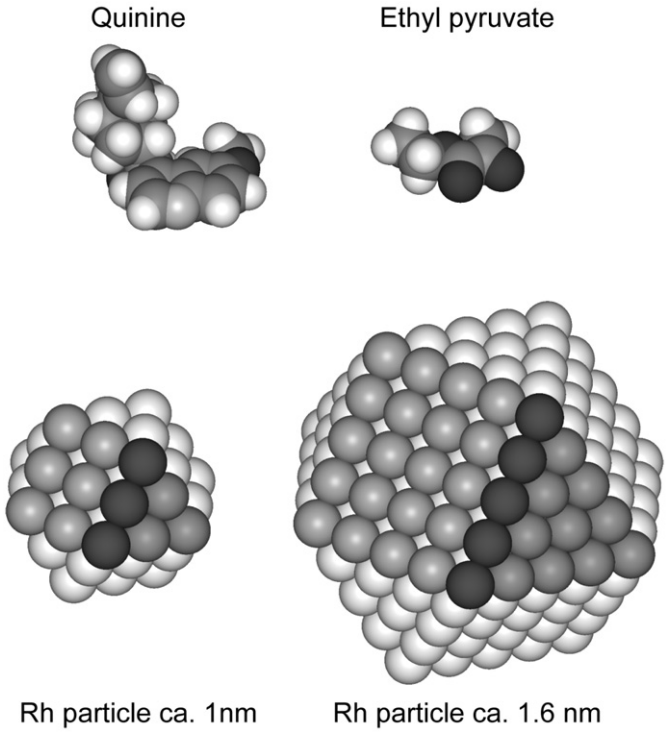

Fig. 11. Two idealized Rh cuboctahedron clusters containing 55 and 309 atoms, and the space-filled models of quinine and ethyl pyruvate; all represented with the same scale.

a crucial role in controlling the structure and properties of small metal particles [74–76] and these effects cannot easily be separated from those mentioned previously.

The activity and enantioselectivity of chirally modified metal catalysts in the hydrogenation of C=O bonds is generally attributed to the presence of metallic surface sites [26,70,77,78]. There is less agreement in the real nature of substrate–modifier interactions leading to enantioselection. In most cases, the mechanistic models assume the adsorption of the chiral modifier and the ketone substrate on neighboring surface sites. Due to the bulkiness of cinchona alkaloids, the substrate–modifier complex would occupy an ensemble of 20–25 metal atoms [79,80]. In the present study the lowest and the highest average metal particle size of Rh/Al_2O_3 catalysts are 0.96 and 1.65 nm (Fig. 2), and the presence of surface Rh oxide after prereduction at 400 °C can be excluded based on the DRIFT measurements. Fig. 11 shows two idealized Rh cuboctahedral particles with 55 and 309 atoms, corresponding to a diameter of ca. 1.0 and 1.6 nm, respectively. The latter crystallite seems to be sufficiently big (25 surface atoms on one face) to accommodate the quinine–ethyl pyruvate interacting complex, which molecules are also presented in Fig. 11 in the same scale. A more detailed consideration is not yet possible, since the mechanism of the reaction on Rh has not been investigated. Assuming similar reaction mechanisms on Pt and Rh, it is very probable that the steric limitation to adsorption of the substrate–modifier complex parallel to the metal surface on small Rh particles plays a role in the low activity and enantioselectivity of Rh/Al_2O_3 catalysts with low Rh loading. According to this assumption, only those Rh particles would give good enantioselectivity, which are big enough to accommodate the substrate–modifier complex, while on smaller particles the enantioselective control of the hydrogenation of the carbonyl group is less efficient or it is not possible at all (leading to racemic product).

The Rh^+ species, detected by the DRIFT measurement of CO adsorption, may indicate the formation of Rh aluminate during the synthesis of Rh/Al_2O_3 catalysts by flame spray pyrolysis at high temperature. These ionic Rh species at the metal–oxide interface (boundary or "adlineation" sites [76]) may also contribute to the striking particle size effect depicted in Fig. 7. Evaluation of this possibility needs an independent evidence for the existence of Rh aluminate in the flame made catalysts.

4. Conclusions

The effect of metal particle size on the catalyst performance, or more general the structure sensitivity in heterogeneous catalysis, is an extensively studied—and debated—field. It is still a challenging task to localize the origin of the phenomenon and separate it from the disturbance caused by, for example, the different impurities in the catalyst systems compared.

Here we applied the flame spray pyrolysis technique to prepare a series of Rh/Al_2O_3 catalysts containing 0.5 to 4.3 wt% Rh. This method provided very small Rh particles with relatively narrow particle size distributions and the best catalyst among them (4.3 wt% Rh) possessed outstanding enantioselectivity in the enantioselective hydrogenation of α-ketoesters. Still, the dramatic drop of reaction rate and enantioselectivity with decreasing particle size (Rh content) cannot simply be attributed to a "classical" particle size effect. Hydrogenation of the substrate in the apolar medium was accompanied by the base-catalyzed aldol condensation leading to strongly adsorbing, large molecular weight byproducts and the extent of this side reaction depends also on the Rh loading. Working at 100 bar we could accelerate the target reaction and minimize the contribution of surface impurities. Under these conditions variation of enantioselectivity with the Rh loading (mean particle size) was still considerable. We assume that the low efficiency of very small Rh particles is mainly due to a geometric effect: these particles cannot adopt the bulky cinchona alkaloid-α-ketoester complex, the formation of which is assumed to be a necessary prerequisite to achieve enantioselection. It seems no advantage of using metal nanoparticles with a particle size of about 2 nm or below, in line with the conclusion of some former studies in enantioselective hydrogenation over Pt [31] and Ir [34].

Acknowledgment

Financial support by the Swiss National Science Foundation (Project No.: 200020-113427) is kindly acknowledged.

References

[1] R. Hess, F. Krumeich, T. Mallat, A. Baiker, J. Mol. Catal. A Chem. 212 (2004) 205.
[2] Y.L. Huang, Y.Z. Li, J.Y. Hu, P.M. Cheng, H. Chen, R.X. Li, X.J. Li, C.W. Yip, A.S.C. Chan, J. Mol. Catal. A Chem. 189 (2002) 219.
[3] H.X. Ma, H. Chen, Q. Zhang, X.J. Li, J. Mol. Catal. A Chem. 196 (2003) 131.
[4] M. Maris, T. Mallat, A. Baiker, J. Mol. Catal. A Chem. 242 (2005) 151.
[5] W. Xiong, H.X. Ma, Y.Y. Hong, H. Chen, X.J. Li, Tetrahedron: Asymmetry 16 (2005) 1449.
[6] E. Toukoniitty, S. Franceschini, A. Vaccari, D.Y. Murzin, Appl. Catal. A 300 (2006) 147.
[7] M. Maris, D. Ferri, L. Konigsmann, T. Mallat, A. Baiker, J. Catal. 237 (2006) 230.
[8] M. Schürch, N. Künzle, T. Mallat, A. Baiker, J. Catal. 176 (1998) 569.
[9] K. Balàzsik, K. Szöri, K. Felföldi, B. Török, M. Bartók, Chem. Commun. (2000) 555.
[10] K. Szőri, K. Balázsik, K. Felföldi, M. Bartók, J. Catal. 241 (2006) 149.
[11] S. Diezi, S. Reimann, N. Bonalumi, T. Mallat, A. Baiker, J. Catal. 239 (2006) 255.
[12] O.J. Sonderegger, G.M.W. Ho, T. Bürgi, A. Baiker, J. Catal. 230 (2005) 499.
[13] E. Schmidt, D. Ferri, A. Baiker, Langmuir 23 (2007) 8087.
[14] E. Schmidt, D. Ferri, A. Vargas, A. Baiker, J. Phys. Chem. C 112 (2008) 3866.
[15] F. Hoxha, T. Mallat, A. Baiker, J. Catal. 248 (2007) 11.
[16] B. Coq, F. Figueras, Coord. Chem. Rev. 180 (1998) 1753.
[17] M. Che, C.O. Bennett, Advances in Catalysis, vol. 36, Academic Press, San Diego, 1989, p. 55.
[18] L. Guczi, G. Petö, A. Beck, Z. Pàszti, Top. Catal. 29 (2004) 129.
[19] O.M. Poltorak, V.S. Boronin, Int. Chem. Ing. 7 (1967) 452.

[20] R. Van Hardeveld, F. Hartog, Surf. Sci. 15 (1969) 189.
[21] B. Coq, F. Figueras, in: A.S. Wieckowski, E.R. Savinova, C.G. Vayenas (Eds.), Catalysis and Electrocatalysis at Nanoparticle Surfaces, Marcel Dekker, New York, 2003, p. 847.
[22] M. Boudart, in: Advances in Catalysis, Academic Press, San Diego, 1969, p. 20.
[23] G.C. Bond, Appl. Catal. A 149 (1997) 3.
[24] S. Azad, M. Kaltchev, D. Stacchiola, G. Wu, W.T. Tysoe, J. Phys. Chem. B 104 (2000) 3107.
[25] R.L. Augustine, S.K. Tanielyan, L.K. Doyle, Tetrahedron: Asymmetry 4 (1993) 1803.
[26] D.Y. Murzin, P. Maki-Arvela, E. Toukoniitty, T. Salmi, Catal. Rev.-Sci. Eng. 47 (2005) 175.
[27] D.Y. Murzin, E. Toukoniitty, React. Kinet. Catal. Lett. 90 (2007) 19.
[28] X. Zuo, H. Liu, D. Guo, X. Yang, Tetrahedron 55 (1999) 7787.
[29] Y. Nitta, T. Kubota, Y. Okamoto, Bull. Chem. Soc. Jpn. 74 (2001) 2161.
[30] Y. Nitta, J. Watanabe, T. Okuyama, T. Sugimura, J. Catal. 236 (2005) 164.
[31] J.T. Wehrli, A. Baiker, M. Monti, H.U. Blaser, J. Mol. Catal. 61 (1990) 207.
[32] G.A. Attard, K.G. Griffin, D.J. Jenkins, P. Johnston, P.B. Wells, Catal. Today 114 (2006) 346.
[33] J.L. Margitfalvi, E. Tàlas, L. Yakhyaeva, E. Tfirst, I. Bertóti, L. Tóth, in: D.G. Morrell (Ed.), Catalysis of Organic Reactions, Dekker, New York, 2003, p. 393.
[34] T. Marzialetti, M. Oportus, D. Ruiz, J.L.G. Fierro, P. Reyes, Catal. Today 133 (2008) 711.
[35] M.A. Keane, Can. J. Chem. 72 (1994) 372.
[36] N. van Vegten, D. Ferri, M. Maciejewski, F. Krumeich, A. Baiker, J. Catal. 249 (2007) 269.
[37] R. Strobel, F. Krumeich, W.J. Stark, S.E. Pratsinis, A. Baiker, J. Catal. 222 (2004) 307.
[38] S.J. Pennycook, Ultramicroscopy 30 (1989) 58.
[39] A. Urakawa, A. Baiker, manuscript in preparation.
[40] P.J. Levy, V. Pitchon, V. Perrichon, M. Primet, M. Chevrier, C. Gauthier, J. Catal. 178 (1998) 363.
[41] A.C. Yang, C.W. Garland, J. Phys. Chem. 61 (1957) 1504.
[42] N. Kaufherr, M. Primet, M. Dufaux, C. Naccache, C. R. Hebdomadaires Des Seances Acad. Sci. Ser. C 286 (1978) 131.
[43] G.M. Alikina, A.A. Davydov, I.S. Sazanova, V.V. Popovskii, React. Kinet. Catal. Lett. 27 (1985) 279.
[44] C.A. Rice, S.D. Worley, C.W. Curtis, J.A. Guin, A.R. Tarrer, J. Chem. Phys. 74 (1981) 6487.
[45] P.B. Rasband, W.C. Hecker, J. Catal. 139 (1993) 551.
[46] R.R. Cavanagh, J.T. Yates, J. Chem. Phys. 74 (1981) 4150.
[47] O. Dulaurent, K. Chandes, C. Bouly, D. Bianchi, J. Catal. 192 (2000) 262.
[48] A. Maroto-Valiente, I. Rodriguez-Ramos, A. Guerrero-Ruiz, Catal. Today 93–95 (2004) 567.
[49] S. Trautmann, M. Baerns, J. Catal. 150 (1994) 335.
[50] J.T. Yates, T.M. Duncan, S.D. Worley, R.W. Vaughan, J. Chem. Phys. 70 (1979) 1219.
[51] J. Rasko, J. Bontovics, Catal. Lett. 58 (1999) 27.
[52] J.P. Wey, W.C. Neely, S.D. Worley, J. Catal. 134 (1992) 378.
[53] P. Basu, D. Panayotov, J.T. Yates, J. Am. Chem. Soc. 110 (1988) 2074.
[54] P. Basu, D. Panayotov, J.T. Yates, J. Phys. Chem. 91 (1987) 3133.
[55] F. Solymosi, M. Pàsztor, J. Phys. Chem. 89 (1985) 4789.
[56] H.F.J. Van't Blik, J. Vanzon, T. Huizinga, J.C. Vis, D.C. Koningsberger, R. Prins, J. Am. Chem. Soc. 107 (1985) 3139.
[57] S.S.C. Chuang, S. Debnath, J. Mol. Catal. 79 (1993) 323.
[58] C.P. Hwang, C.T. Yeh, Q.M. Zhu, Catal. Today 51 (1999) 93.
[59] C. Wong, R.W. McCabe, J. Catal. 119 (1989) 47.
[60] K. Dohmae, T. Nonaka, Y. Seno, Surf. Interface Anal. 37 (2005) 115.
[61] H.C. Yao, W.G. Rothschild, J. Chem. Phys. 68 (1978) 4774.
[62] D. Duprez, J. Barrault, C. Geron, Appl. Catal. 37 (1988) 105.
[63] D. Duprez, G. Delahay, H. Abderrahim, J. Grimblot, J. Chim. Phys. Phys.-Chim. Biol. 83 (1986) 465.
[64] J.C. Summers, S.A. Ausen, J. Catal. 58 (1979) 131.
[65] A. Borodzinski, M. Bonarowska, Langmuir 13 (1997) 5613.
[66] M. von Arx, T. Mallat, A. Baiker, Top. Catal. 19 (2002) 75.
[67] D. Ferri, S. Diezi, M. Maciejewski, A. Baiker, Appl. Catal. A 297 (2006) 165.
[68] Z.M. Liu, X.H. Li, P.L. Ying, Z.C. Feng, C. Li, J. Phys. Chem. C 111 (2007) 823.
[69] J.M. Bonello, R.M. Lambert, N. Künzle, A. Baiker, J. Am. Chem. Soc. 122 (2000) 9864.
[70] M. Studer, H.U. Blaser, C. Exner, Adv. Synth. Catal. 345 (2003) 45.
[71] H.U. Blaser, H.P. Jalett, F. Spindler, J. Mol. Catal. A Chem. 107 (1996) 85.
[72] C.O. Bennett, M. Che, J. Catal. 120 (1989) 293.
[73] T. Stace, Nature 331 (1988) 116.
[74] C.R. Henry, Surf. Sci. Rep. 31 (1998) 235.
[75] G. Haller, D.E. Resasco, Adv. Catal. 36 (1989) 173.
[76] K. Hayek, R. Kramer, Z. Paal, Appl. Catal. A 162 (1997) 1.
[77] T. Mallat, E. Orglmeister, A. Baiker, Chem. Rev. 107 (2007) 4863.
[78] M. Bartók, Curr. Org. Chem. 10 (2006) 1533.
[79] A. Vargas, T. Bürgi, A. Baiker, J. Catal. 226 (2004) 69.
[80] K.E. Simons, P.A. Meheux, S.P. Griffiths, I.M. Sutherland, P. Johnston, P.B. Wells, A.F. Carley, M.K. Rajumon, M.W. Roberts, A. Ibbotson, Recl. Trav. Chim. Pays-Bas 113 (1994) 465.